ELSEVIER

Journal of Contaminant Hydrology 29 (1997) 41–58

JOURNAL OF
Contaminant
Hydrology

Laboratory-scale analysis of aquifer remediation by in-well vapor stripping 2. Modeling results

Michael J. Pinto [a,*], Haim Gvirtzman [b], Steven M. Gorelick [a]

[a] *Department of Geological and Environmental Sciences, Stanford University, Stanford, CA 94305, USA*
[b] *Institute of Earth Sciences, The Hebrew University of Jerusalem, Jerusalem, 91904, Israel*

Received 10 April 1996; revised 10 November 1996; accepted 10 November 1996

Abstract

The removal of volatile organic compounds (VOCs) from groundwater through in-well vapor stripping has been demonstrated by Gonen and Gvirtzman (1997, J. Contam. Hydrol., 00: 000–000) at the laboratory scale. The present study compares experimental breakthrough curves with those predicted by three-dimensional numerical simulation of VOC transport, volatilization, and removal. We are able to sufficiently model the behavior of the laboratory system by assuming an isotropic, homogeneous hydraulic conductivity field and uniform linear retardation of the VOCs. The exponential reductions in concentrations of trichlorethylene, chloroform, and toluene were well represented by the simulation model. Local disparities between experimental and simulated breakthrough curves appear to result primarily from differences between the actual and estimated initial concentrations, and secondarily from differences in the actual and modeled flow field. Our analysis suggests that the in-well vapor stripping process is understood at the laboratory scale. The model developed for this work provides a sound basis for current analysis at the field scale.

Keywords: Recirculating wells; In-well vapor stripping; Volatile organic compounds; Air-lift pumping

* Corresponding author.

PII S0169-7722(96)00092-7

1. Introduction

This is the second in a series of two papers dealing with the removal of volatile organic compounds (VOCs) from groundwater through in-well vapor stripping, analyzed at the laboratory scale. The companion paper (Gonen and Gvirtzman, 1997) presents results for an in-well vapor stripping experiment conducted at the laboratory scale. This paper presents numerical modeling results of that experiment. The reader is referred to Gvirtzman and Gorelick (1992) for a detailed discussion of the concept of in-well vapor stripping, and to the companion paper for the conditions under which the laboratory experiment was conducted. What follows in this introduction is a brief overview of in-well vapor stripping and a summary of the laboratory experiment. In addition to laboratory experiments, field demonstrations of the approach are currently under way.

The concept of in-well vapor stripping for the removal of volatile organic compounds from groundwater was introduced by Gvirtzman and Gorelick (1992). In situ remediation is accomplished by injection of air into a well, using a combined technique of air-lift pumping with a form of VOC vapor stripping.

The process by which remediation occurs is depicted in Gonen and Gvirtzman (1997, Fig. 1). Groundwater is lifted above the water table using air-lift pumping. During the air-lift process, VOCs partition from the groundwater into the air bubbles in the well. The partially treated groundwater, which is air-lifted to a designated height above the water table, is then allowed to infiltrate back to the aquifer. A flow recirculation cell is established within the aquifer, because groundwater is both extracted from and infiltrates back to the aquifer. The VOC-laden air is extracted with a vacuum or is otherwise ventilated, and the partially cleaned water infiltrates back to the aquifer. Detailed information about the kinetics of contaminant mass transfer associated with air-lift pumping have been given by Gvirtzman and Gorelick (1992).

The effectiveness of in-well vapor stripping recently has been explored under controlled conditions in laboratory experiments by Gonen and Gvirtzman (1997). An aquifer model of 2 m length (hereafter referred to simply as the aquifer) was constructed, into which three dissolved VOCs (chloroform, toluene, and trichloroethylene (TCE)) were introduced. An in-well vapor stripping system was installed within the aquifer (Gonen and Gvirtzman, 1997, Fig. 2). Groundwater was extracted by air-lift pumping from the center of the aquifer, transported to a recharge pond near one end of the aquifer, and allowed to infiltrate back to the water table, causing recirculation to be induced within the aquifer. Concentrations of VOCs were measured in groundwater samples from eight monitoring wells, each containing three sampling intervals, collected at various time intervals during the 48 h period over which the experiment was conducted. By the end of the experiment, initial concentrations were reduced by over 90% in some cases.

Numerical simulation of the Gonen and Gvirtzman laboratory experiment is the subject of this paper. Numerical simulation is used to answer a fundamental question: Can the observed breakthrough curves be explained through simulation of the primary transport processes believed to be active at the laboratory scale? We aim to identify the appropriate flow and transport conditions and parameters of the laboratory in-well vapor stripping system (e.g. hydraulic conductivity, linear retardation factor, initial conditions, boundary conditions, and stripping ratio), to answer this question.

2. Numerical simulation of the laboratory experiment

2.1. Flow modeling

2.1.1. Equations

Recirculating flow is created within the aquifer by extraction of contaminated groundwater from one location and by infiltration of partially treated groundwater back to the aquifer. The positions of the recharge pond and extraction wells are depicted in Fig. 1.

Flow through the entire system consists of a saturated component and an unsaturated component. Unsaturated flow occurs as water percolates downward from the recharge zone to the water table. The water table responds by forming a saturated mound. In our modeling approach, we have chosen to ignore unsaturated flow, as it is limited in its spatial extent and the water percolates relatively quickly to the water table. Therefore, we considered only saturated flow, with recharge applied directly to the water table over an area approximately equal to the area of the recharge pond.

The equation employed for modeling steady saturated flow is (Bear, 1979)

$$K_h\left(\frac{\partial^2 h}{\partial x_1^2}+\frac{\partial^2 h}{\partial x_2^2}\right)+K_v\frac{\partial^2 h}{\partial x_3^2}+q_s=0 \tag{1}$$

where K_h is horizontal hydraulic conductivity, K_v is vertical hydraulic conductivity, q_s is volumetric flux of water per unit volume of aquifer (positive for inflow), x_1 and x_2 are coordinate axes aligned with the sides of the tank, and x_3 is the vertical coordinate axis. We have used a steady flow model because, based on simulations and observation, the flow system reaches steady state within a few minutes, which is short in relation to the duration of the experiment. We initially assumed that hydraulic conductivity is anisotropic, as packing and settling of sand during the construction of the aquifer may have induced some degree of anisotropy. As discussed below, the system is very well described as isotropic.

Dirichlet boundary conditions are applied at the two sides of the aquifer with storage reservoirs (Fig. 1 and Fig. 2). Zero-flow boundary conditions are applied along the other

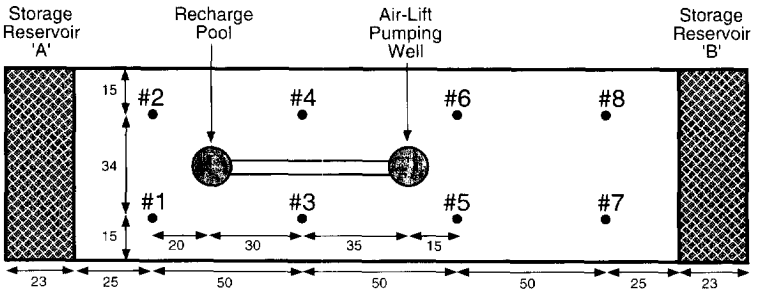

Fig. 1. Schematic representation of the laboratory experiment. Monitoring wells are numbered 1–8. All distances are in centimeters.

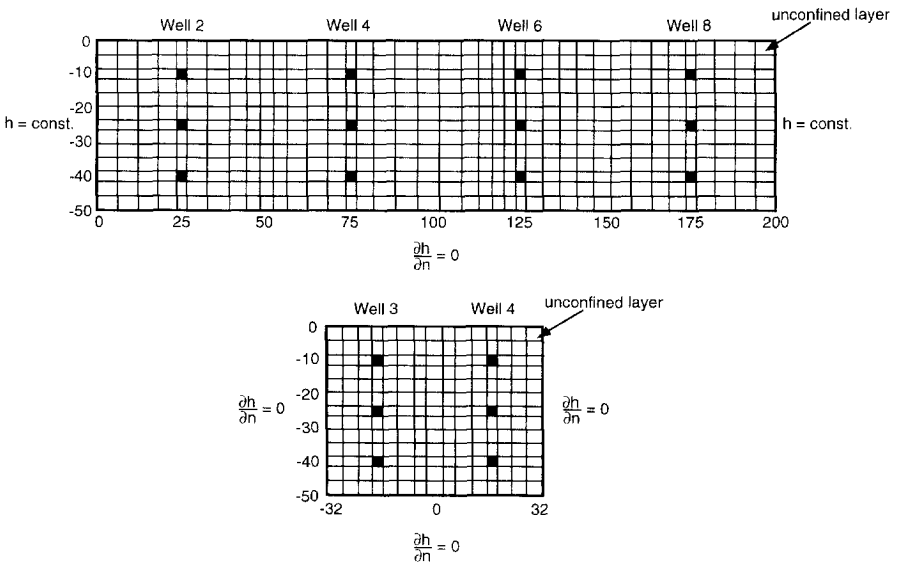

Fig. 2. Discretization of the simulation domain along two vertical planes. The cells corresponding to sampling intervals are shaded in gray and are included here for reference. Boundary conditions for the flow model are shown next to their respective boundaries.

two sides and the bottom of the aquifer. The aquifer is treated as unconfined, so that the transmissivity of the uppermost layer of the discretized flow model is allowed to vary during solution of the flow equation.

2.1.2. *Simulation of flow*

Saturated flow was simulated with MODFLOW, the modular three-dimensional finite-difference groundwater flow model of the US Geological Survey (McDonald and Harbaugh, 1988). Flow parameters used in the model are presented in Table 1.

The simulation domain is discretized into 15 rows, 41 columns, and 13 layers, for a total of 7995 model cells (Fig. 2). The grid spacing is approximately uniform in each dimension. Finer spacing is used in the vicinity of the sampling intervals of the observation wells, and coarser spacing is used between the sampling intervals.

Table 1
Flow parameters

Parameter	Symbol	Unit	Value
Horizontal hydraulic conductivity	K_h	$m\,s^{-1}$	1.74×10^{-3}
Vertical hydraulic conductivity	K_v	$m\,s^{-1}$	5.80×10^{-4} to 1.74×10^{-3}
Total porosity	θ	–	0.30
Pumping rate	Q	$m^3\,s^{-1}$	1.25×10^{-5}
Recharge flux	I	$m\,s^{-1}$	8.7×10^{-4}
Recharge area	A	m^2	1.75×10^{-2}

Recharge to the aquifer is simulated by applying a uniform recharge flux of 8.7×10^{-4} m s^{-1} to the top of nine model cells. The total area covered by these cells is 1.44×10^{-2} m^2 (the actual area of the circular recharge pool in the aquifer is approximately 1.75×10^{-2} m^2.

Extraction of groundwater from the aquifer occurs along the entire length of the extraction screen, which is fully penetrating. Extraction was modeled by applying a uniform extraction rate per unit length of the extraction screen. The head along the extraction well is nearly uniform (Fig. 3). Extraction is simulated by 13 constant-flux cells, with a combined flow rate of 1.25×10^{-5} m^3 s^{-1} (0.75 l min^{-1}). Because the extraction screen could also be modeled as a constant head boundary, we also investigated that modeling approach. We found that, on average, the difference in flow rate at any given extraction cell for the two methods is about 3.5%. Transport simulations based on the constant-flux and the constant-head approaches show extremely little difference. Therefore, we have retained the constant-flux condition in our simulations.

Constant head values were assigned to the boundaries at each side containing a water reservoir, but we did not have measured values for the water level in each water storage reservoir. Therefore, it was necessary to first simulate flow by modeling the water storage reservoirs as high-permeability zones, whose hydraulic conductivity was 100 times greater than that of the aquifer. Zero-flow boundaries were imposed around the water storage reservoirs. The modeling grid was modified to account for the actual size of the storage reservoirs. The values of head in the cells corresponding to the storage reservoirs were found to be nearly constant. These values of head were then assigned to constant-head boundaries for subsequent flow and transport simulations. For the case of uniform, isotropic hydraulic conductivity, the flow rate into or out of storage reservoir A is 3.75×10^{-7} m^3 s^{-1} (32.4 l day^{-1}), and the flow rate into or out of storage reservoir B is 1.4×10^{-9} m^3 s^{-1} (0.12 l day^{-1}) (Fig. 1). These flow rates are 3.0% and 0.01%, respectively, of the pumping rate at the extraction well. The net flow rate from each storage reservoir is zero.

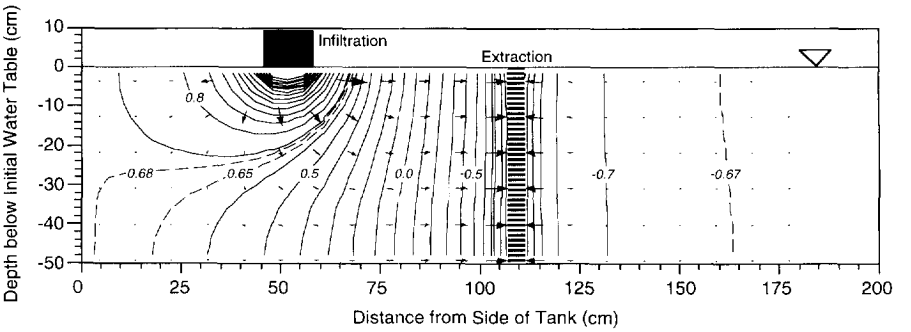

Fig. 3. Steady-state total head and groundwater velocities. This vertical profile is taken along the plane of symmetry of the system. The contour interval for total head is 0.1 cm. Velocity vectors are scaled according to the magnitude of the velocity at selected locations. The water table before air-lift pumping is provided for reference. Infiltration from the recharge pond at the top of the tank (not shown) is schematically depicted as vertical flow owing to gravity drainage.

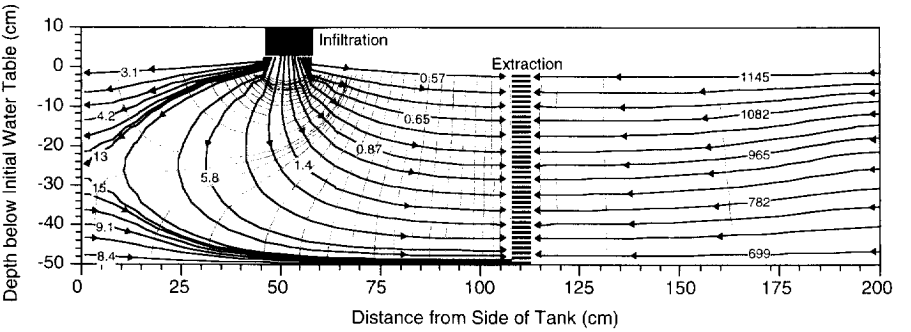

Fig. 4. Pathlines with travel times from the recharge pond and the storage reservoirs to the air-lift pumping well. This vertical profile is taken along the plane of symmetry of the system. Travel times are in hours. Contours of total head (gray) are presented for reference.

The value of horizontal hydraulic conductivity used in the model is 1.74×10^{-3} m s^{-1} (150 m day^{-1}). This value is based on flow measurements conducted through packed columns and through the aquifer itself (Gonen and Gvirtzman, 1997). As vertical hydraulic conductivity was not measured, we considered values ranging from 5.80×10^{-4} to 1.74×10^{-3} m s^{-1} (50–150 m day^{-1}). This corresponds to ratios of horizontal to vertical hydraulic conductivity in the range 1–3. We did not expect this ratio to be much greater than unity, as the sand used in the tank is fairly uniform in its grain size and sphericity, and the tank was carefully packed.

Simulated steady-state heads for a flow system with uniform, isotropic hydraulic conductivity are shown in Fig. 3. This figure depicts head along the vertical plane of symmetry. Water levels were not measured during the actual experiment, so we do not have observed values of total head against which to compare our simulated results. The average simulated drawdown at the extraction well is about 0.012 m, the average simulated drawup at the recharge pond is 0.022 m, the drawup in storage reservoir A is 0.0068 m, and the drawdown in storage reservoir B is 0.0067 m. Calculated groundwater velocities are superimposed on the map of head in Fig. 3. Velocities have been computed using an effective porosity of 0.30, which is equal to the total porosity. Groundwater velocities are relatively high between the recharge pond and the extraction well, and diminish rapidly with distance.

Pathlines were calculated using MODPATH (Pollock, 1989). Pathlines are shown for particles traveling along the plane of symmetry (Fig. 4). The time of travel between the recharge pond and the extraction well for selected pathlines is also presented in Fig. 4. There is substantial variation in travel time along different pathlines. The shortest travel time is approximately 2000 s (0.6 h), while in the portion of the aquifer furthest from both injection and extraction, travel times exceed 3.6×10^{6} s (1000 h).

2.2. *Transport modeling*

2.2.1. *Equations*

The governing equation employed for modeling equilibrium-controlled sorptive contaminant transport within a saturated flow regime is the advective–dispersive equation

with retardation (Bear, 1979):

$$R\frac{\partial C}{\partial t} = \frac{\partial}{\partial x_i}\left(D_{ij}\frac{\partial C}{\partial x_j}\right) - \frac{\partial}{\partial x_i}(v_i C) + \frac{q_s}{\theta_{\text{eff}}}C_s \quad i,j = 1,2 \tag{2}$$

where C is the concentration of dissolved contaminant in the aqueous phase, C_s is the concentration of fluid sources and sinks, R is the retardation factor, D_{ij} is the hydrodynamic dispersion tensor (which includes molecular diffusion), v_i is the component of the linear groundwater velocity in the ith direction, q_s is the volumetric rate of fluid injection or extraction per unit volume of aquifer, and θ_{eff} is effective porosity.

The partitioning of VOCs from the aqueous phase to the vapor phase during a single pass of groundwater through the in-well vapor stripping system is accounted for in the model through a stripping ratio. This ratio can be expressed in the following form:

$$s = \frac{C_{\text{intake}} - C_{\text{outlet}}}{C_{\text{intake}}} \tag{3}$$

where C_{outlet} is the concentration of a particular VOC in infiltrating groundwater, C_{intake} is the concentration of the VOC in extracted groundwater, and s is the stripping ratio for that compound (TCE, chloroform, or toluene) which reflects the removal of VOCs by in-well vapor stripping. A stripping ratio of unity indicates complete stripping of VOCs from the aqueous phase, whereas a stripping ratio of zero indicates that no VOCs have been removed from the aqueous phase by in-well vapor stripping. Stripping ratios were determined from controlled air-lift pumping experiments in which concentrations at the top and bottom of the extraction well were measured (Gonen and Gvirtzman, 1997, Table 4).

Additional modeling assumptions made are, as follows:

1. Partially treated groundwater returns to the aquifer as soon as it is extracted from the aquifer. We estimate that it takes less than 5 min for water from the recharge pool to infiltrate to the water table. This estimate is based upon the distance from the recharge pond to the initial water table (0.5 m), vertical hydraulic conductivity, effective porosity, and a hydraulic gradient of unity for gravity drainage from the recharge pool. This period of time is small in relation to the time required to extract one pore volume from the entire system (slightly more than 4 h).
2. The stripping ratios remain constant during the entire experiment, regardless of changes in concentration of VOCs dissolved in groundwater. This is consistent with Henry's Law.
3. Volatilization of VOCs from the water table into the unsaturated zone is negligible. If volatilization of VOCs from the saturated zone into the unsaturated zone were significant, a decreasing trend in initial concentration vs. depth below the water table should have been observed in the multilevel monitoring wells at the onset of the experiment. Such a trend was not observed.
4. Losses of VOCs from the storage reservoirs by volatilization have not been included in the model. These losses are considered to be small in relation to the amount of VOCs removed by air stripping. The very small reduction in VOC concentrations at storage reservoir B during the experiment indeed suggests that volatilization from the storage reservoirs can be neglected.

5. Adsorption of VOCs to the Plexiglas well casing or the sides of the tanks has not been incorporated into the model. Some VOCs have a tendency to sorb to Plexiglas. Given that the areas of the air-lift pumping well and tank walls (approximately 2.7 m^2) are small in relation to the total surface area of the aquifer solids (approximately 1500 m^2), we consider the mass sorbed onto the Plexiglas to be relatively minor.
6. Hydrodynamic dispersion can be modeled by using a single value of longitudinal dispersivity, a single value of transverse dispersivity, and a single value of the molecular diffusion coefficient throughout the system.

We do not assume that volatilization of VOCs from the air-lift well to the recharge pond, or from the recharge pond to the water table through the unsaturated zone, is negligible. For each constituent we have considered two possible stripping ratios. The lower stripping ratio is from careful measurements during controlled air-lift experiments by Gonen and Gvirtzman (1997). The higher stripping ratio incorporates possible additional losses, which, for each constituent, are estimated to be a few per cent of the VOC concentration after air-lifting. The stripping ratios range from 32 to 44% for in-well stripping only; by incorporating additional losses, the range may be as high as 38–51%. These stripping ratios are low because the air-lift distance was only about 1 m. It is a simple matter to obtain much higher stripping ratios in the field, as the distance over which water is air-lifted is considerably greater than in the laboratory. At existing field demonstrations, stripping ratios exceed 90% (Gilmore et al., 1996).

2.2.2. *Simulation of transport*

Parameters used in the transport model are summarized in Table 2. We considered three values of longitudinal dispersivity: 0, 0.01, and 0.05 m. Transverse dispersivity was set to one-tenth the value of longitudinal dispersivity. A molecular diffusion coefficient of 5×10^{-10} m^2 s^{-1} was incorporated into the transport model, as molecular diffusion may not be negligible at the laboratory scale. We used only one value of the retardation factor for each constituent, as the retardation factor was experimentally determined to fall within a very narrow range.

The initial concentration distribution was generated by a block approach. The aquifer was divided into 24 major blocks of approximately equal dimensions, with a sampling point at or near the center of each block. The initial concentration of a constituent at a

Table 2
Transport parameters

Parameter	Symbol	Unit	Chloroform	TCE	Toluene
Longitudinal dispersivity	α_L	m	0.01–0.05	0.01–0.05	0.01–0.05
Ratio of transverse to longitudinal dispersivity	α_T / α_L	m	0.1	0.1	0.1
Molecular diffusion	D^*	$m^2 s^{-1}$	5.0×10^{-10}	5.0×10^{-10}	5.0×10^{-10}
Distribution coefficient	K_d	$m^3 kg^{-1}$	1.7×10^{-4}	2.3×10^{-4}	2.1×10^{-4}
Retardation factor	R	–	1.23	1.40	1.30
Effective porosity	θ_{eff}	–	0.30	0.30	0.30
Stripping ratio	s	–	0.32, 0.38	0.44, 0.51	0.39, 0.46

particular sampling point was assigned to all the cells within the block containing the sampling point. This approach does not capture short-range spatial variations that are present in the actual initial concentration field, but it is consistent with the measured value of total initial dissolved mass in the system based on laboratory calculations (Gonen and Gvirtzman, 1997), whereas other methods (e.g. inverse distance weighting methods) are not. As the short-range spatial variations that are initially present are rapidly erased by recirculation and mixing over a large volume of the aquifer, incorporating these variations into the modeling of the initial concentration field is not essential. It is important, however, to use the correct total initial mass, as the concentration within a large volume of the aquifer becomes fairly uniform in a short period of time, and this concentration depends upon the total initial dissolved mass. An exception to this is the end of the tank near storage reservoir B, where recirculation is extremely sluggish, and mixing is very limited.

The concentrations of constituents in the influent from the constant head boundaries are specified over time according to measurements of contaminant concentrations from samples taken from the storage reservoirs during the experiment (Fig. 5). Concentrations in storage reservoir B change very slightly, as there is relatively little flow into and out of this reservoir. The reason why storage reservoir B has notably lower concentrations than storage reservoir A is a consequence of the way in which the tank was filled. The

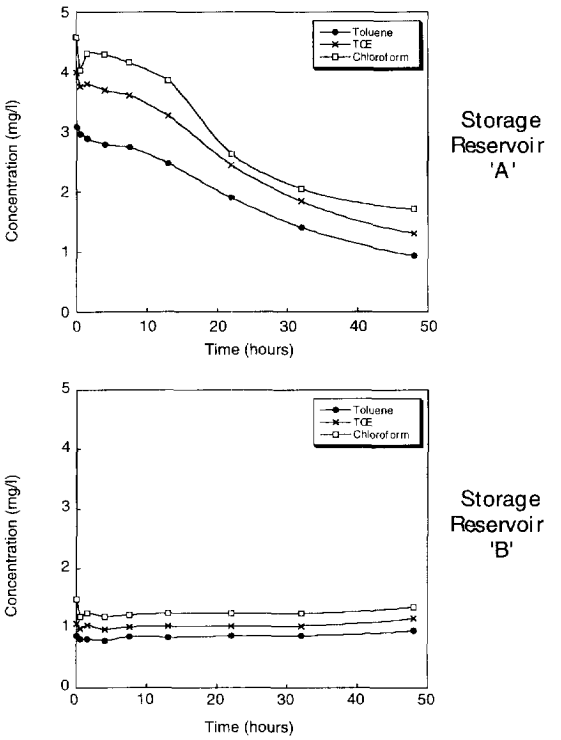

Fig. 5. Constituent concentrations vs. time for the two storage reservoirs.

tank was first filled with clean water. Contaminated water was then introduced into storage reservoir A. The water level in storage reservoir B was maintained at a slightly lower level than in storage reservoir A to induce flow from reservoir A to reservoir B. Only 1.65 pore volumes of contaminated water were introduced into the aquifer through reservoir A. This quantity was insufficient for expelling clean water from storage reservoir B and its environs. This explains not only the lower concentrations observed in storage reservoir B, but also some of the low concentrations observed at the middle and lower horizons of Well 8 during the course of the experiment.

The numerical simulation model MT3D (Zheng, 1992), which incorporates a mixed Eulerian–Lagrangian approach to the solution of the advective–dispersive equation, was used to simulate transport. We amended MT3D to accommodate fluid sources whose concentrations vary with each time step. We made an additional modification that allows us to relate, through the stripping ratios, the concentration of extracted groundwater to that of injected groundwater at each time step of the simulation.

The modeling grid used for simulation of contaminant transport is identical to the one used for the flow model. A uniform simulation time step was used in each transport

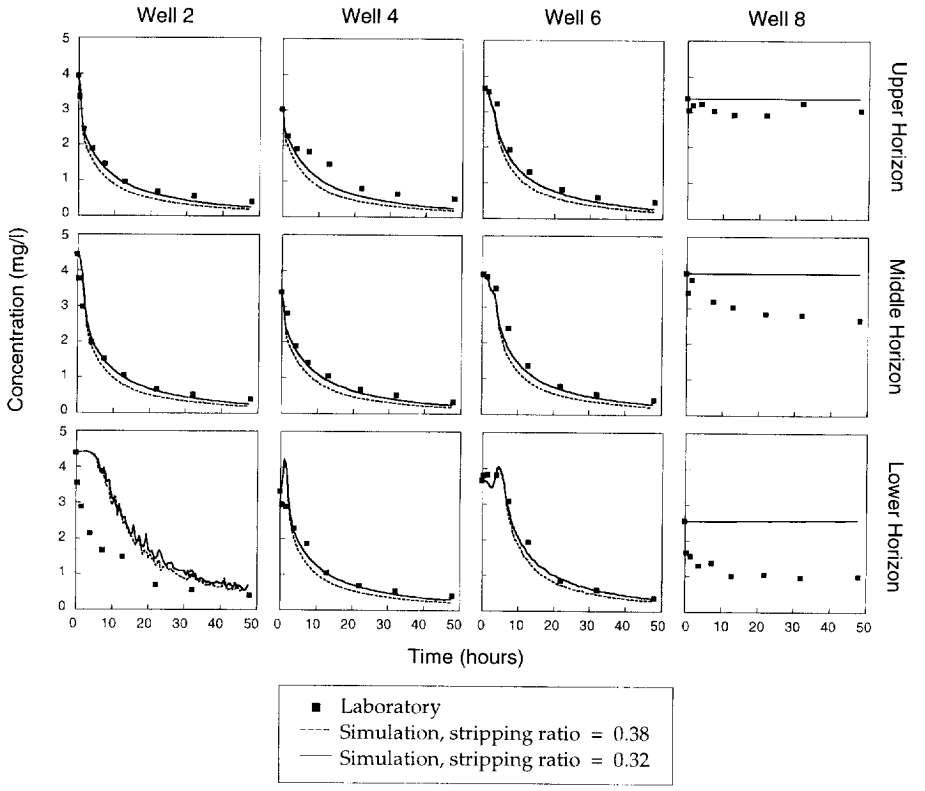

Fig. 6. Simulated vs. experimental breakthrough curves for chloroform. A retardation factor of 1.23 and a longitudinal dispersivity of 0.01 m were used in the numerical simulations.

simulation. For simulations which do not incorporate retardation, the time step used was 147 s (4.08×10^{-2} h). Differences in the time steps for the different VOCs reflect differences in retardation factors for different constituents. The mass balance error was approximately 0.5–1%.

3. Comparison of experimental and simulation results

Experimental and simulated breakthrough curves for chloroform, toluene, and TCE are shown in Fig. 6, Fig. 7 and Fig. 8, respectively. Breakthrough curves are shown only for Wells 2, 4, 6, and 8. These results are based on a flow system with homogeneous, isotropic hydraulic conductivity and a longitudinal dispersivity of 0.01 m. The two simulated breakthrough curves on each plot represent the two values of the stripping ratio for each constituent presented in Table 2. Contour plots along two vertical cross-sections at 13 h and 48 h are shown in Fig. 9, Fig. 10 and Fig. 11. One vertical cross-section contains Wells 2, 4, 6, and 8; the other contains Wells 3 and 4 (see Fig. 1

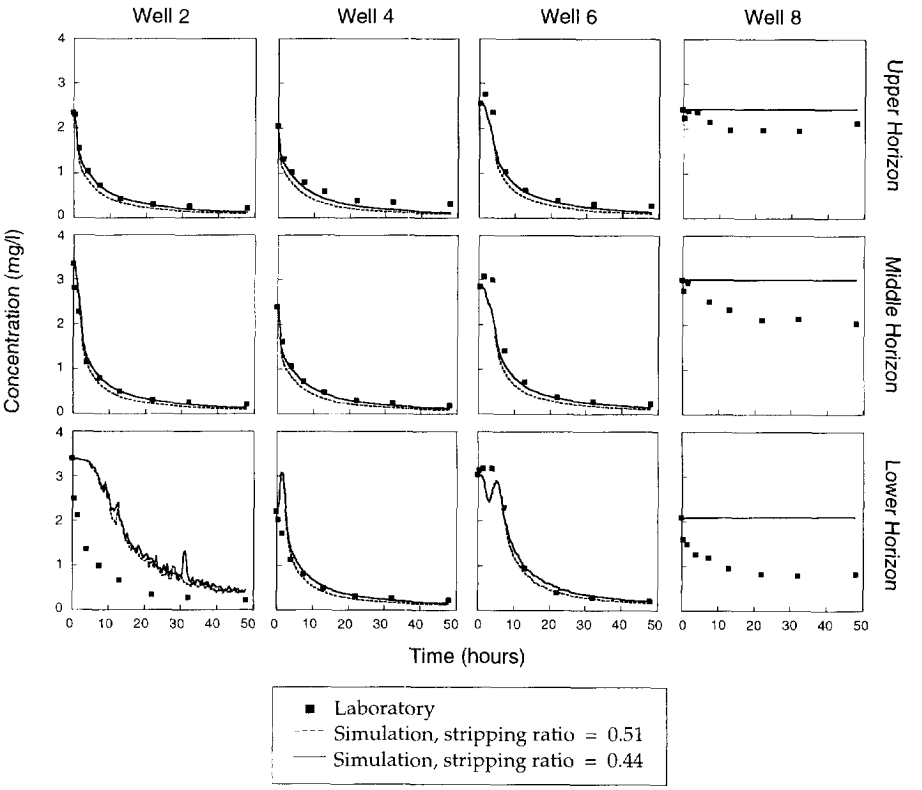

Fig. 7. Simulated vs. experimental breakthrough curves for trichloroethylene (TCE). A retardation factor of 1.40 and a longitudinal dispersivity of 0.01 m were used in the numerical simulations.

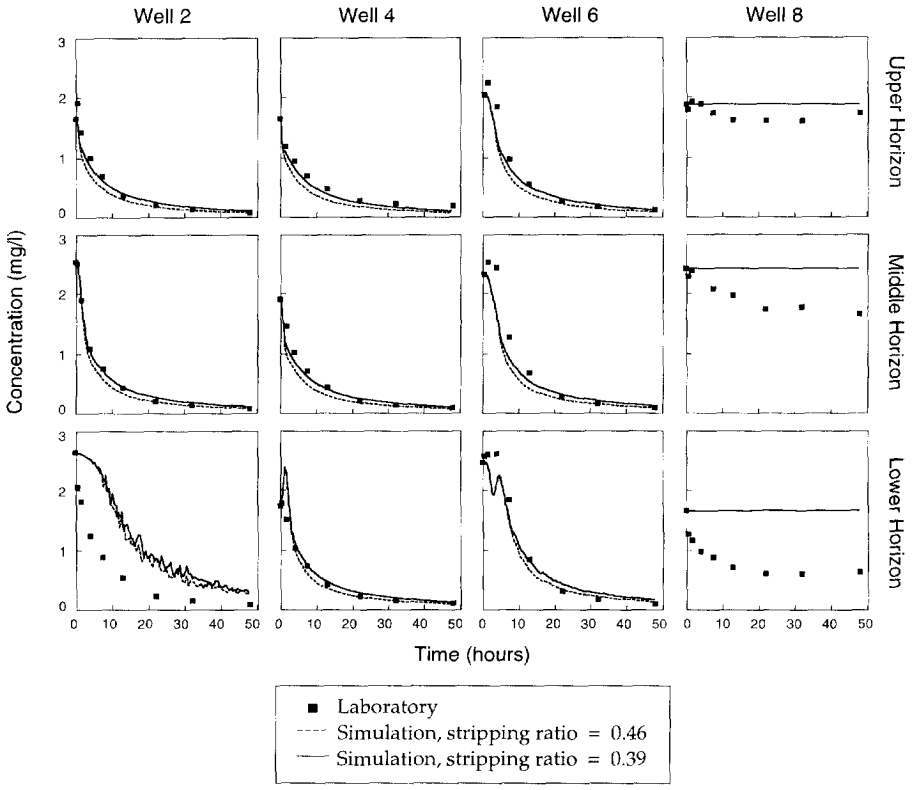

Fig. 8. Simulated vs. experimental breakthrough curves for toluene. A retardation factor of 1.30 and a longitudinal dispersivity of 0.01 m were used in the numerical simulations.

for the locations of these wells). Corresponding experimental concentrations are also presented for comparison.

The correspondence between experimental and simulated concentration is very good for each of the constituents. The fit is usually better for the lower stripping ratio than for the higher stripping ratio for a given constituent, although we expected the fit to be better for the higher stripping ratio, which incorporates VOC losses from the recharge pond and the vadose zone. It is possible that we have overestimated VOC losses from the recharge pond and vadose zone, resulting in excessive estimates of the higher stripping ratio.

There are some exceptions to the high degree of agreement between the experimental and simulated concentrations. There is a large discrepancy between the experimental and simulated concentrations at Well 8. Concentrations at Well 8 do not display the same behavior as observed at other wells, as the effects of recirculation have not extended to this well by the end of the experiment. The concentration histories at Well 8 primarily reflect the initial concentrations in the vicinity of Well 8. The disparity between the experimental and simulated concentrations is due to a mismatch between the actual and

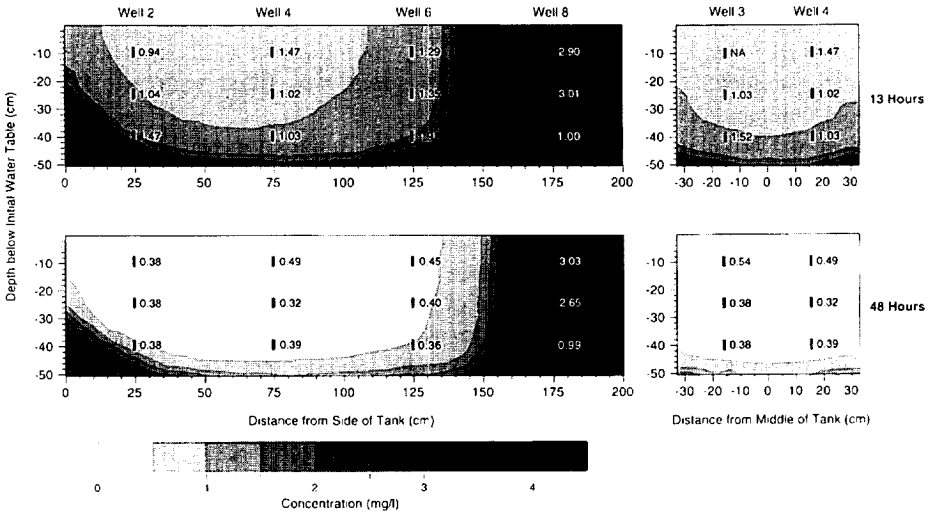

Fig. 9. Simulated isoconcentration contours for chloroform along longitudinal and transverse vertical cross-sections at 13 and 48 h from the beginning of the experiment. The longitudinal cross-section contains Wells 2, 4, 6, and 8. The transverse cross-section contains Wells 3 and 4. Concentrations are expressed in milligrams per liter. The contour interval is 0.5 mg l^{-1}. Experimental concentrations are denoted next to the sampling intervals for comparison. The stripping ratio used here is 0.32.

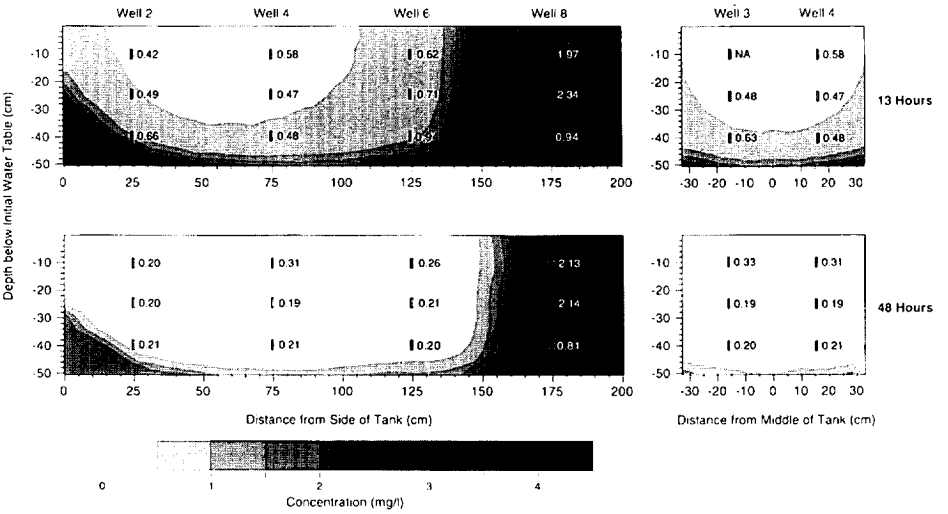

Fig. 10. Stimulated isoconcentration contours for trichloroethylene (TCE) along longitudinal and transverse vertical cross-sections at 13 and 48 h from the beginning of the experiment. The longitudinal cross-section contains Wells 2, 4, 6, and 8. The transverse cross-section contains Wells 3 and 4. Concentrations are expressed in milligrams per liter. The contour interval is 0.5 mg l^{-1}. Experimental concentrations are denoted next to the sampling intervals for comparison. The stripping ratio used here is 0.44.

estimated initial concentrations. The relatively low concentrations observed at the lower horizon of Well 8 during the experiment probably are indicative of clean water that was not flushed completely from the tank when the tank was filled with just 1.65 pore volumes of contaminated water.

Some of the simulated breakthrough curves (e.g. upper horizon of Well 4) show notable deviations from the experimental breakthrough curves during the first several hours of the experiment. These deviations are due to the mismatch between actual initial concentrations and the estimated initial concentrations used in the simulations.

There is a relatively poor correspondence between the experimental and simulated breakthrough curves at the lower horizon of Well 2. The effects of recirculation are observed much sooner in experimental breakthrough curves than in the simulated breakthrough curves (Fig. 6, Fig. 7 and Fig. 8). We attribute this disparity to differences between the actual flow field and the modeled flow field. The simulated breakthrough curves are rather choppy compared with other simulated breakthrough curves. Transport simulators such as MT3D, which are based on the method-of-characteristics, typically produce breakthrough curves which appear jagged when the number of particles at a given model cell varies substantially with time. There appears to be greater variation in the number of particles at the lower horizon of Well 2 than at other well horizons, thus explaining the simulated breakthrough behavior.

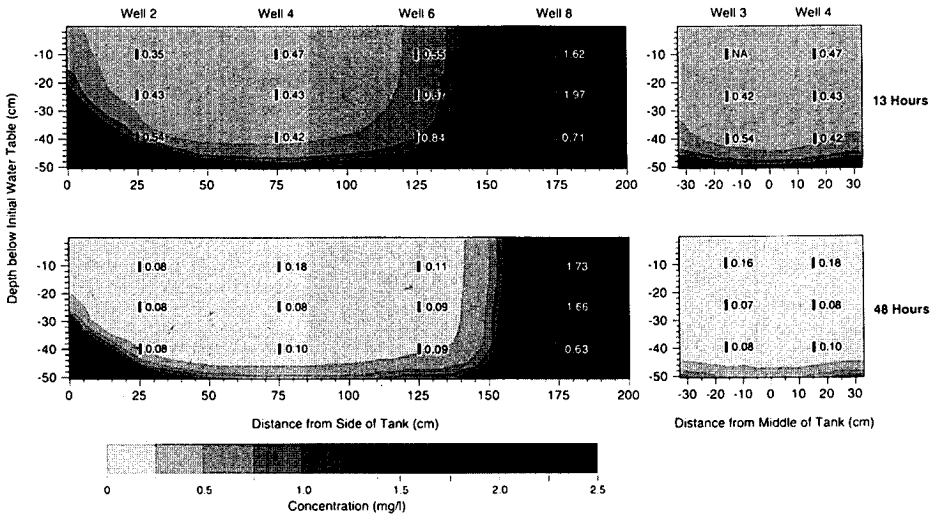

Fig. 11. Simulation isoconcentration contours for toluene along longitudinal and transverse vertical cross-sections at 13 and 48 h from the beginning of the experiment. The longitudinal cross-section contains Wells 2, 4, 6, and 8. The transverse cross-section contains Wells 3 and 4. Concentrations are expressed in milligrams per liter. The contour interval is 0.25 $mg l^{-1}$. Experimental concentrations are denoted next to the sampling intervals for comparison. The stripping ratio used here is 0.39.

4. Sensitivity analysis

We conducted sensitivity analyses for two parameters: vertical hydraulic conductivity and longitudinal dispersivity. The simulation results are rather insensitive to variations in the values of these two parameters.

As stated above, we considered values of vertical hydraulic conductivity ranging from 5.80×10^{-4} to $1.74 \times 10^{-3}\ \mathrm{m\,s^{-1}}$, or ratios of vertical to horizontal hydraulic conductivity in the range 1–3. We were able to constrain the upper bound on the ratio of vertical to horizontal conductivity to be approximately 2.5. We conducted particle-tracking studies for one well (the upper interval of Well 8). This well was not affected by injection and recirculation of treated water during the experiment, and thus was a good candidate for particle-tracking analysis. If the ratio of vertical to horizontal conductivity is greater than approximately 2.5, then the travel time to the upper horizon of Well 8 for a particle originating at the recharge pond is less than 48 h, i.e. the total duration of the

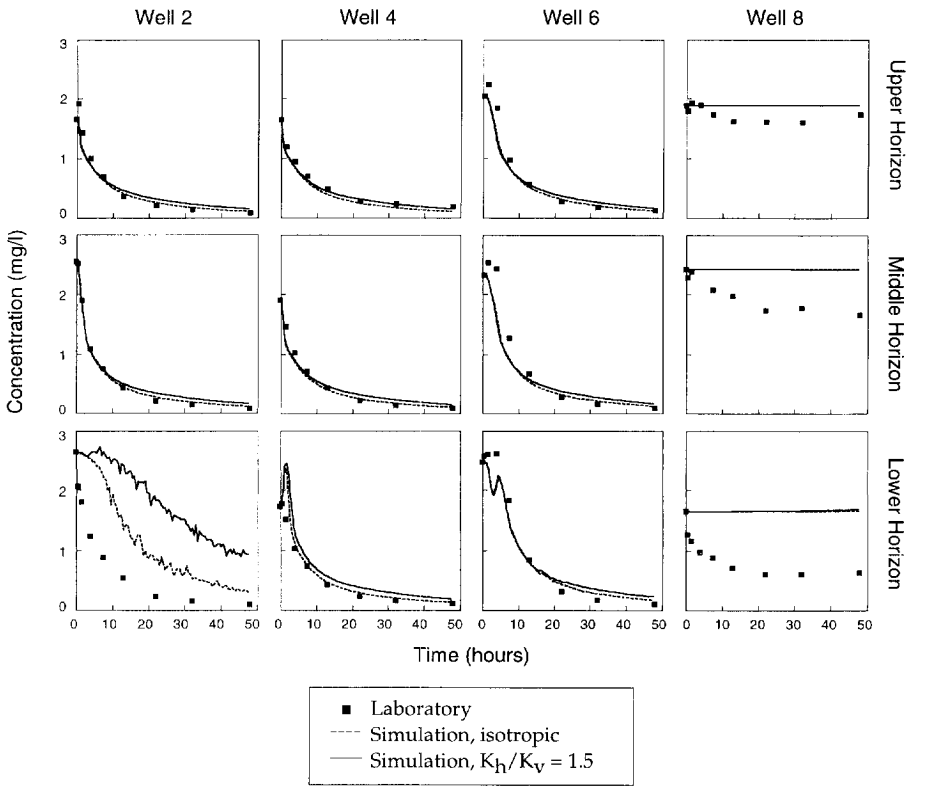

Fig. 12. Sensitivity analysis of simulated breakthrough curves to vertical hydraulic conductivity. The simulation and experimental results shown here are for toluene. A retardation factor of 1.30, longitudinal dispersivity of 0.01 m, and stripping ratio of 0.39 were used in the simulations. The term K_h / K_v in the legend denotes the ratio of horizontal to vertical hydraulic conductivity. Horizontal hydraulic conductivity (K_h) was maintained at $1.74 \times 10^{-3}\ \mathrm{m\,s^{-1}}$.

experiment. This method therefore establishes an approximate upper limit on the ratio of hydraulic to vertical conductivity.

We simulated transport of toluene for two ratios of horizontal to vertical conductivity (Fig. 12). The ratios used are unity (isotropic) and 1.5. There is very little difference in the simulation results, especially where flow is dominantly horizontal. One notable exception is the lower horizon of Well 2. The breakthrough curve for a ratio of 1.5 is markedly worse than that for a ratio of unity. It appears, then, that an isotropic hydraulic conductivity model is the best one for this study, and therefore we did not explore higher values of anisotropy.

To analyze the effect of changes in longitudinal dispersivity, we compared two simulations for toluene (Fig. 13). One simulation used a longitudinal dispersivity of 0.01 m; the other used a longitudinal dispersivity of 0.05 m. The ratio of transverse to longitudinal dispersivity in both cases was 0.1. There is little change in the breakthrough curves for the different values of longitudinal dispersivity. Changes are more pronounced in the lower interval of the monitoring wells. The fit of the breakthrough curves for a longitudinal dispersivity of 0.01 m is marginally better than that of the break-

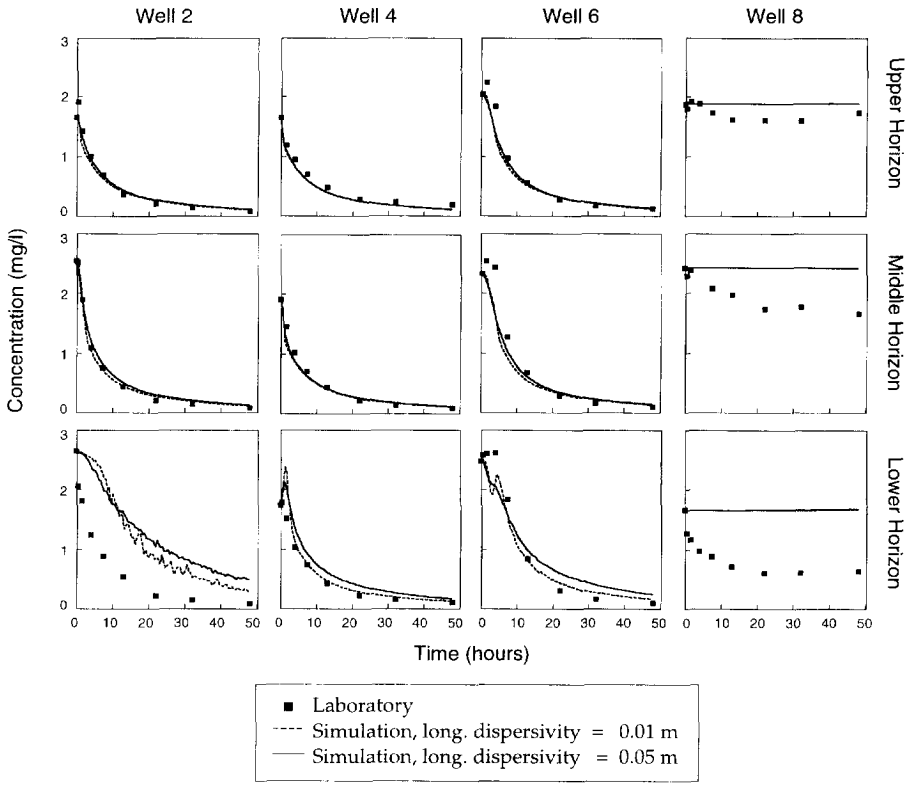

Fig. 13. Sensitivity analysis of simulated breakthrough curves to longitudinal dispersivity. The simulation and experimental results shown here are for toluene. A retardation factor of 1.30 and a stripping ratio of 0.39 were used in the simulations.

through curves for a longitudinal dispersivity of 0.05 m for the lower horizons. We conclude that the modeling results are relatively insensitive to longitudinal dispersivity, and that using a nominal value of 0.01 m is appropriate for this study.

5. Summary and conclusions

We have simulated the in-well vapor stripping laboratory experiment conducted by Gonen and Gvirtzman (1997) by three-dimensional flow and transport modeling. Flow within the aquifer was considered to be steady in all simulations. Experimentally derived values were used for horizontal hydraulic conductivity, effective porosity, and retardation factors. We considered a range of values for vertical hydraulic conductivity and dispersivity, as these were not determined experimentally. Two stripping ratios, one corresponding to vapor stripped from the well and the other incorporating possible additional volatilization losses, were selected for the simulation analyses. The range of stripping ratios attained in the laboratory is notably less than can be attained in the field, because air-lifting distances are considerably less in the laboratory.

Flow and transport models used in this study reasonably explain the experimental results. There is usually very good agreement between simulated and experimental breakthrough curves for each of the VOCs under consideration. Reductions in simulated concentrations resulting from recirculation and in-well VOC stripping were indeed observed at Wells 2–6, whereas reductions were not observed at Well 8. In addition, at those wells where concentration reductions were observed during the laboratory experiment, the model predicts similar reductions (approximately 90% of the average initial concentrations) over the 48 h duration of the experiment. Disparities between experimental and simulated breakthrough curves appear to result primarily from differences between the actual and estimated initial concentrations, and secondarily from differences in the actual and modeled flow field.

The modeling approach used here can easily be extended to model data collected under field conditions. It can also be used to estimate the extent and degree of remediation of actual field sites, although it may be necessary to incorporate kinetic parameters in the model, as rate-limited mass transfer may become dominant in field cases for which the time scales involved are long. A field experiment has been conducted at Edwards Air Force Base in California to assess the applicability of this remediation method at the field scale. The same processes appear to apply at both the laboratory and field scales; however, the stripping ratios achieved in the field exceeded 90% (Gilmore et al., 1996).

Acknowledgements

Funding for this study was provided by the Office of Research and Development, US Environmental Protection Agency, under Agreement R-81975 through the Western Region Hazardous Substance Research Center. The content of this study does not necessarily represent the view of the Agency. This work was also supported by the Arid

Zone VOC Integrated Demonstration Program of the US Department of Energy. Computer facilities were provided by a grant from the Hewlett-Packard Company, with additional support from the National Science Foundation (Grant BCS-8957186).

References

Bear, J., 1979. Hydraulics of Groundwater. McGraw–Hill, New York, NY.

Gilmore, T.J., Pinto, M.J., White, M.D., Ballard, S., Gorelick, S.M., Taban, O. and Spane, F.A., 1997. Preliminary Performance Assessment of the In-Well Vapor-Stripping System. Pacific Northwest National Laboratory, Richland, WA (October 1996).

Gonen, O. and Gvirtzman, H., 1997. Laboratory-scale analysis of aquifer remediation by in-well vapor stripping: 1. Laboratory results. J. Contam. Hydrol., 29, 23–39.

Gvirtzman, H. and Gorelick, S., 1992. The concept of in situ vapor stripping for removing VOCs from groundwater. J. Transp. Porous Media, 8: 71–92.

McDonald, M.G. and Harbaugh, A.W., 1988. Modeling techniques. In: A Modular Three-Dimensional Finite Difference Ground-Water Flow Model, Book 6. Scientific Software Group, Washington, DC.

Pollock, D.W., 1989. Documentation of computer programs to compute and display pathlines using results from the U.S. Geological Survey modular three-dimensional finite-difference ground-water flow model. US Geol. Surv. Open File Rep. 89-381.

Zheng, C., 1992. MT3D: a modular three-dimensional transport model for simulation of advection, dispersion, and chemical reaction of contaminants in groundwater systems, Version 1.5.5. S.S. Papadopulos and Assoc., Bethesda, MD.